Study of the molecular basis of Congenital Disorders of Glycosylation using yeast as a model organism

Human Biology Final Degree Project 2021

Author: Neus Guiu Gonzalez[1]

Director: Oriol Gallego Moli[1,2]

Academic tutor: J. Miguel López-Botet Arbona[1,2,3]

[1]Facultat de Ciències de la Salut i de la Vida, Universitat Pompeu Fabra

[2]Departament de Ciències Experimentals i de la Salut, Universitat Pompeu Fabra (DCEXS-UPF)

[3]Institut Hospital del Mar d'Investigacions Mèdiques (IMIM)

Keywords: *S. Cerevisiae*, Congenital Disorder of Glycosylation (CDG), Rft1, N-linked Glycosylation, Fluorescence Microscopy.

Character count: 14171

Summary

Congenital Disorders of Glycosylation (CDG) are a group of inherited human disorders caused by defects on protein glycosylation. Rft1-CDG is a form of CDG caused by mutations in the gene *RFT1*. Rft1 is a conserved protein essential for the N-linked glycosylation pathway in the ER. The subcellular localization of Rft1 has not been explored experimentally, although it is crucial for Rft1 function and protein glycosylation. The purpose of this research is to characterize the subcellular distribution of Rft1 and to investigate the molecular defects caused by Rft1-CDG mutations using *S. Cerevisiae* as a model organism. To answer this question, we investigated the colocalization between GFP tagged Rft1 and several mCherry tagged subcellular structures using fluorescence microscopy. We found that wild-type GFP-Rft1 localizes in the Endoplasmic Reticulum (ER), the Golgi Apparatus, endosomes and mitochondria. The Rft1-CDG mutations introduced to the GFP-Rft1 strain were R179E, M446V, I340K, G320D, I340R and R75C. Results show that in Rft1-R179E mutant yeast strain, the localization of Rft1 within the cell remains similar to the wild-type. However, the intensity distribution of the GFP-Rft1 fluorescent signal in mutants Rft1-R179E and Rft1-I340K is altered and the duplication time of these particular mutants and Rft1-G320D mutant is increased. Our results provide, for the first time, observations of the impact of Rft1-CDG mutations that can contribute identifying the molecular basis of human CDG.

Introduction

Congenital Disorders of Glycosylation (CDG) are a group of genetic diseases with multisystemic manifestations caused by defects on the glycosylation pathways (1). CDG are classified according to the glycosylation pathway that is affected: N-linked glycosylation, O-linked glycosylation, combined N- and O-linked glycosylation, and lipid glycosylation defects (1)(2).

N-linked glycosylation is a conserved posttranslational modification of proteins in eukaryotic cells (3). This process involves the assembly of a tetradecasaccharide substrate ($Glc_3Man_9GlcNAc_2$) on a lipid carrier, dolichol-linked oligosaccharide (DLO). Then, the tetradecasachharide substrate is transferred to selected asparagine (Asn) residues of peptides (3). The formation of the DLO is a multistep process that starts in the cytoplasmic side of the membrane of the endoplasmic reticulum (ER) with the synthesis of the $Man_5GlcNAc2$-PP-dolichol intermediate (M5-DLO) (4). The following steps of the N-linked glycosylation pathway require the translocation of M5-DLO across the membrane, in such a manner that the oligosaccharides face the lumen of the ER. Then, the synthesis of the fully assembled DLO continues and the M5-DLO is extended to mature M9-DLO by adding four mannose and three glucoses. Finally, the oligosaccharide from the lipid carrier DLO is transferred to the amide group of selected Asn residues (3) (**Fig. 1**).

N-linked protein glycosylation defect Rft1-CDG, also called CDG-In, is a form of CDG caused by mutations in the gene *RFT1* (5). The first Rft1-CDG patient was identified by Haeuptle MA and colleagues in 2008 (5). Psychomotor retardation, hypotonia, seizures, hepatomegaly, and coagulopathy were the predominant signs and symptoms (5). Lately, a pathogenic point mutation in *RFT1* gene causing CDG was identified in a child of Hospital Sant Joan de Déu (HSJD) in Barcelona. The patient carries the Rft1-R179E mutation and the clinical phenotype comprises typical CDG symptoms.

Rft1 is a membrane protein first discovered in *Saccharomyces Cerevisiae* (*S. Cerevisiae*) in an attempt to identify p53-like proteins in yeast (6). The Rft1 protein was discovered as a mutant that requires wild-type p53 for its viability (6). Rft1 has been suggested to localize in the ER of yeast and human cells based on indirect observations from genetic experiments. The subcellular localization of Rft1 is fundamental for its function and protein glycosylation (4). Nonetheless, Rft1 localization has not been explored experimentally (4). The human Rft1 protein shares 22% identity with its yeast ortholog (5). Yeast and human Rft1 are functionally redundant (5), and both are essential for

normal protein N-linked glycosylation (4). However, Rft1 role in this pathway remains enigmatic.

At first, Rft1 was proposed to catalyze the transmembrane movement of M5-DLO across the ER membrane in *S. Cerevisiae* (**Fig. 1**) (4). Evidence showed that the absence of Rft1 prevented N-linked glycosylation and resulted in an accumulation of M5-DLO in the cytoplasmic side of the ER membrane, suggesting that Rft1 has a flippase activity (4). However, *in vitro* studies with reconstituted vesicles challenged this interpretation and reported that in the absence of Rft1, flipping of M5-DLO still occurred (7). Some biochemical studies suggest that Rft1 may act as a chaperone that controls the lateral distribution of DLOs in the ER and by doing that regulates their access to the flippase (8)(9).

Here we present a study, in collaboration with HSJD of Barcelona, that aims to contribute to the understanding of the molecular basis of glycosylation disorders. Using CRISPR/Cas9 novel technology, we generated and characterized yeast cells harboring either of 6 Rft1 mutants with clinical interest, including Rft1-R179E. We analyzed the subcellular localization of yeast Rft1 in wild-type strains and in Rft1-CDG mutant strains using fluorescence microscopy (**Fig. 2**). The results of this study show that some Rft1-CDG mutations reduce yeast viability and that Rft1 distribution in yeast cells can be affected by point mutations causing CDG.

Results

Generation of Rft1-CDG mutant strains

In order to understand the role of Rft1 in CDG, we generated six Rft1-CDG mutant yeast strains using CRISPR/Cas9 technology. The introduced point mutations were: R179E, M446V, I340K, G320D, I340R and R75C (**Fig. 3A-F**). The first four mutations were made in haploid yeast cells, expressing Rft1 tagged with Green Fluorescence Protein (GFP). Haploid yeast cells with mutations Rft1-I340R and Rft1-R75C did not grow in the plates with the corresponding antibiotic resistance marker, suggesting that these two mutations can compromise yeast viability. Hence, mutations Rft1-I340R and Rft1-R75C were introduced in diploid yeast cells, expressing only one copy of GFP tagged Rft1 in the genome. Mutants were validated by PCR using mutation-specific primers and confirmed by sequencing (**Fig. 3G**).

Characterization of Rft1-CDG mutant strains

To study if the mutations introduced in the Rft1 gene could have an effect on the fitness rate of yeast cells, we analyzed how Rft1 wild-type cells and Rft1-CDG mutant cells were

growing over time. Growth curves of the strains were generated by measuring the Optical Density (OD) at different time intervals. Taking into account that *S. Cerevisiae* duplication time is approximately 1.5 hours (10), our results showed that cells carrying the mutation Rft1-R179E show a 1.3-fold increase in the duplication time, when compared to the wild-type strain. Mutations Rft1-I340K and Rft1-G320D also lead to a reduction of yeast growth, resulting in duplication times that are 2 times and 1.6 times the duplication time of the wild type strain, respectively (**Fig. 4A-B**). These data shows that the growth rate of yeast is affected by the Rft1-CDG mutations, suggesting that some Rft1-CDG mutations may hamper the functionality of Rft1.

Subcellular distribution of GFP-Rft1

As explained before, subcellular compartmentalization is fundamental for the N-linked glycosylation pathway. To test if the subcellular distribution of Rft1 is affected by mutations causing CDG, we analyzed the localization of wild-type and Rft1-CDG mutants by fluorescence microscopy. Live-cell imaging showed that wild-type GFP-Rft1 forms bright spots within the cell. Regarding the mutant strains, the GFP-Rft1 distribution in some of them is different from wild-type GFP-Rft1, while in some others, the distribution remains similar. On the one hand, in Rft1-R179E and Rft1-I340K mutants, GFP-Rft1 does not form evident bright GFP spots and is distributed homogeneously in the cell. This phenotype is specially seen in Rft1-I340K mutant. On the other hand, in Rft1-M446V and Rft1-G320D mutant strains, GFP-Rft1 forms bright GFP spots, similar to the ones observed in wild-type Rft1 (**Fig. 5**). These differences in the GFP-Rft1 distribution insinuate that point mutations in the *RFT1* gene may result in changes on Rft1 localization, which may lead to defects on the Rft1 functionality and/or alterations in Rft1 expression levels.

Colocalization analysis of GFP-Rft1 and different cell markers

It has been shown that Rft1 is important for N-linked glycosylation pathway occurring in the ER (4). Nevertheless, so far it has not been described where Rft1 localizes in the cell. To investigate the localization of Rft1 in the cell, specific genes of different subcellular structures were tagged with a red fluorescence label. For that, we introduced a C-terminal mCherry tag in strains expressing GFP-Rft1. Subcellular structures were tagged endogenously by homologous recombination or by exogenous tagging using plasmids. Endogenous cell markers used were: Sec7 (Trans Golgi Network), Sec13 (ER Exit Sites), Alo1 (Mitochondria) and Pex11 (Peroxisomes). Exogenous cell markers used were: HDEL (ER) and Ape1 (Selective autophagy). Additionally, the dye FM4-64 was used to label endosomes with red fluorescence. We conducted a colocalization analysis

using dual-color fluorescence microscopy in strains expressing GFP-Rft1 and any of the above-mentioned cell markers.

Live-cell imaging showed that wild-type Rft1 is located in several subcellular structures. The subcellular structure where the biggest fraction of the Rft1 protein localizes is in the ER Exit Sites (ERES), with 13.3 ± 2.2 % of the GFP-Rft1 signal colocalizing with the mCherry-Sec13 signal in this particular structure. Rft1 colocalizes as well with Sec7 (7.8 ± 1.8 %), FM464 (5.6 ± 3.7 %) and Alo1 (7.2 ± 2.2 %), markers of Trans Golgi Network (TGN), endosomes and mitochondria, respectively. Negligible levels of GFP-Rft1 were detected in other subcellular structures, such as peroxisomes (Pex11) or autophagosome vesicles (Ape1) (**Fig. 6A-B**). Our data localized approximately 40% of Rft1 protein, nonetheless, the colocalization analysis failed to localize the majority of Rft1. Therefore, the localization of most of the Rft1 protein remains to be explored.

To check whether the subcellular localization of Rft1 is affected when mutations causing CDG are introduced, we conducted the same colocalization assay carried out in the wild-type strain, but now using Rft1-CDG mutant strains. In the live-cell images of the strain carrying the Rft1-R179E mutation, the one found in the child from HSDJ, we can see that GFP-Rft1 colocalizes with the same mCherry tagged subcellular structures as the wild-type strain; ERES (Sec13), TGN (Sec7), endosomes (FM4-64) and mitochondria (Alo1) Additionally, GFP-Rft1 shows little colocalization with mCherry-HDEL, a marker of ER (**Fig. 6C**).

The results from the colocalization analysis reveal that wild-type Rft1 protein is localized simultaneously in different subcellular structures, including ERES, TGN, endosomes and mitochondria. Apart from that, when Rft1-CDG mutations are introduced in *S. Cerevisiae*, Rft1 protein distributes similar to the wild-type strain, although colocalization between GFP-Rft1 and mCherry tagged subcellular structures in Rft1-CDG mutant yeast strains has only been observed by live-cell imaging and has not been quantified yet. This quantification analysis will be addressed in the future to explore if the fraction of Rft1 localizing in each of the above-mentioned structures in the Rft1-R179E mutant is different from the wild-type strain.

Discussion

The functional conservation of Rft1 in eukaryotes enables to study the molecular basis of human CDG in unicellular eukaryotic organisms, such as *S. Cerevisiae*. As part of this study, we generated a GFP-Rft1 yeast strain, making it possible to localize the Rft1 protein in living cells by fluorescence microscopy. As a means to draw a picture on the

molecular basis of CDG, we engineered strains expressing point mutations in the *RFT1* gene, which allowed us to study how clinically relevant Rft1 behaves.

Results of this study show that wild-type Rft1 is needed for yeast to grow in the best conditions, emphasizing the importance of the *RFT1* gene, conserved between yeast and human. The fluorescence microscopy results demonstrated that, GFP-Rft1 changes the distribution in some of the mutants, although quantification of the Rft1 expression levels is desirable for future work. The observed impact of mutations Rft1-R179E and Rft1-I340K on the intensity distribution of the GFP-Rft1 fluorescent signal correlates with the alterations detected on the fitness rate of these yeast strains. This fact could be associated with a more severe clinical course of human CDG.

Another promising finding of this study is that, in line with recent studies conducted in *Trypanosoma Brucei* (11), yeast Rft1 does not localize exclusively in the ER, as originally proposed (4). This study localizes Rft1 in several subcellular structures of *S. Cerevisiae*, such as in the Golgi Apparatus, endosomes and mitochondria. According to our colocalization analysis a major fraction of Rft1 localizes in the ERES rather than in ER. This results can be consistent with the idea that, although the transfer of the initial oligosaccharide to proteins occurs in the ER, glycoproteins enter the cis-Golgi and the mature glycan is then fully synthetized in the Golgi Apparatus (12). We speculate that the localization of Rft1 in different subcellular structures might be due to the implication of Rft1 in more cellular processes, and not only in the N-linked glycosylation pathway. This may explain why the majority of Rft1 has not been localized yet. It is a question of our future research to investigate the fraction of Rft1 that localizes in subcellular structures that remain unexplored in the present study, such as in the *cis*-Golgi. Alternatively, since single filters were used for the imaging and the exposure time for the GFP-channel was long, the fact that the biggest fraction of Rft1 has not been localized in this study could simply mean that Rft1 is a highly dynamic protein. Therefore, by the time the GFP channel was imaged and the filter cube was switched to mCherry, Rft1 had already moved within the cell.

From our results, it remains unclear to which degree the minor observed changes in the localization of Rft1 are attributed to the Rft1-CDG mutations, since only preliminary results are available regarding the quantification of the colocalization in the Rft1-CDG mutant yeast strains. However, if Rft1-CDG mutations do not seem to impact the localization of Rft1, an interesting topic to be explored would be if Rft1-CDG mutations have an impact on Rft1 interactome. This will be addressed in our future research using protein Cross-Linking coupled Mass Spectrometry (XL-MS).

Altogether, our findings open new questions regarding the localization of yeast Rft1 and its ortholog in human cells Further live-cell studies need to be performed to fully understand the role of Rft1 in the N-linked Glycosylation pathway and possibly in other biological pathways. This study provides, for the first time, observations of the impact of Rft1-CDG mutations that can contribute to understand the biology behind the expanding group of metabolic disorders due to defects in the glycosylation pathways.

Materials and Methods

Plasmids and strain construction

All constructs were generated by conventional PCR and the yeast transformation protocol indicated below (13). Tagging of genes was made either by homologous recombination of the corresponding genes with PCR amplified cassettes (endogenous markers) or by transformation of the entire plasmid (exogenous markers). When endogenous markers were transformed, the plasmids encoding the tag contained the S2/S3 primer annealing site for PCR-targeting, as proposed by Janke et al in 2008 (14). Plasmid pOG044 was used to N-terminally tag with GFP and plasmid pOG201 was used to C-terminally tag with 3xmCherry. Plasmids pOG105 and pOG190 were used to express exogenously mCherry tagged HDEL and Ape1, respectively.

Yeast cells expressing a N-terminal GFP-Rft1 were engineered. To obtain Rft1-CDG mutant strains the point mutations were incorporated in the *RFT1* gene using CRISPR/Cas9 Technology (15).

For the localization analysis, specific genes of different subcellular structures were tagged with C-terminal mCherry in strains expressing GFP-Rft1. Endogenous cell markers used were: Sec7 (Trans Golgi Network), Sec13 (ER Exit Sites), Alo1 (Mitochondria) and Pex11 (Peroxisomes). Exogenous cell markers used were: HDEL (ER) and Ape1 (Selective autophagy). The dye FM4-64 was used to label endosomes with red fluorescence. See Tables S1 and S2 for a complete list of the plasmids and strains used in this study.

Yeast transformation

Parental strains were grown in Yeast Extract-Peptone-Dextrose (YPD) medium (Formedium) at 30ºC overnight. Next morning, cultures were diluted and grown for 5 hours up to exponential phase (OD_{600} = 1). Cells were pellet at 2.500 rpm for 3 min at room temperature (RT) and washed twice with MiliQ water. After discarding the supernatant, cells were resuspended in 500 μL of LP buffer (40% Polyethylene glycol (PEG), 0.1M Lithium acetate (LiAc) dissolved in TE). Strains were transformed with 40

μL of PCR product, in the case of endogenous markers, or with 100-200 ng of the plasmid miniprep, in the case of exogenous markers. Also, 5μL of salmon sperm DNA were added to increase specificity. Cells were resuspended and incubated for 40 min in a water bath at 42ºC. Then, cells were washed twice with 700 μL of 1X TE and centrifuged again at 2.500 rpm for 3 min at RT. For selection with amino acid depletion (exogenous markers), cells were resuspended in 30 μL of 1X TE and plated on plates lacking the amino acid of choice. For selection with antibiotic resistance (endogenous markers), cells were cultured overnight in YPD at 30ºC and plated next morning on plates containing the antibiotic of interest. All positive colonies were confirmed by imaging.

Diploid strains generation

For the mutant strains that could not be validated in haploid yeast cells, a diploid strain expressing GFP-Rft1 in one allele was generated. The haploid strain expressing GFP-Rft1 (OGY1127, mating type a) was crossed with another haploid strain of the opposite mating type that had a non-tagged Rft1 (OGY002, mating type α) (**Table S1**). The mating between these two strains was done in a YPD plate. Then, both diploid cells and cells expressing two GFP-Rft1 alleles were selected in histidine dropout medium plates. To select exclusively the diploid cells, single colonies were isolated and observed in the microscope. Diploid cells were confirmed by PCR to be heterozygous for GFP tagged Rft1.

Mutant generation

As mentioned above, Rft1-CDG mutant strains were engineered by CRISPR/Cas9. Benchling's option for CRISPR experiments was used to design the single-guide RNA (sgRNA), the donor DNA and to find PAM sequences. The sgRNA and donor DNA were chosen among all the possible sequences considering the On-target and Off-target values or the proximity to the desired place of cut in the genomic sequence. To prevent the Cas9 from cutting the DNA once the mutation of interest is introduced, the PAM sequence or the sgRNA were also mutated. To introduce the Rft1-CDG mutations, the GFP-Rft1 yeast strain was transformed following the classic protocol with 100-200 ng of the plasmid containing the sgRNA (**Table S1**) and at least 1 μg of the donor DNA, already annealed with a temperature gradient in a thermocycler. Positive colonies were selected in YPD plates containing cloNat to a final concentration of 100 μg/mL, validated by PCR and confirmed by sequencing.

Growth analysis

All cultures were done in YPD, 30ºC and 220 rpm. Strains were grown during 8 h and subsequentially diluted to OD_{600}= 0.00049. After 17 h, cultures reached the logarithmic phase and OD_{600} = 1. Then, cultures were diluted to OD_{600} = 0.2 and OD_{600} was measured after 7.5 h in a UV-Vis Spectrophotometer (Thermo Scientific). Duplication time (Td) of each strain was calculated according to the following formula of exponential growth:

$$Td = t\ (log2\ (\frac{N(t)}{No})$$

Microscope setup

A Nikon Inverted Microscope Eclipse Ti2-E equipped with a PlanApo λ 100x/1.45 objective lens (Nikon) and a sCMOS Zyla Camera (Andor) with a pixel size of 64.5 nm was used. Cells were excited with SpectraX Lumencor LED system. For GFP channel, the excitation/emission filter cube used was LF488-C (475/35;525/45; Di02-R88). For mCherry channel, the excitation/emission filter cube used was LED-mCherry-A (578/21;641/75; Di01-596). The acquisition software used was Micro-Manager. A schematic representation of the microscope setup is shown in **Fig. 2.**

Live-cell imaging

Prior to imaging, cells were grown in YPD at 30ºC overnight. Next morning, cells were diluted in LF (Yeast Nitrogen Base without amino acids and without Riboflavin and Folic Acid (Formedium)) and grown for 5 hours up to exponential phase (OD_{600} = 1). Cells were attached to a 96-well imaging plate previously coated with Concanavalin A. After 15 min incubation at room temperature, cells were washed twice with LF and 50 μL of LF were added on top. For the labeling of endosomes, attached cells were incubated for 5 min with 50 μL of 8 μM FM4-64 dye, prior to washing with LF. Strains were imaged at RT.

For each sample we acquired 6 fields of view. The field of view was imaged sequentially in the mCherry and GFP channel, switching the filter cubes, and then it was moved to a different region, to avoid photobleaching. Exposure time for GFP channel was 1000 ms and for mCherry channel was 100 ms, except for Ape1, which was 50 ms. The shift in the images between GFP and mCherry channels due to the use of single filters was computationally corrected.

Image analysis

ImageJ software was used for general manipulation of images. To take representative images and compare them, the background was subtracted in all images and the same brightness and contrast were applied in the GFP channel, to make the GFP-Rft1 signal comparable between strains. In the mCherry channel, the brightness and contrast were adjusted for each subcellular marker, nevertheless, the values were maintained between strains. The quantification of colocalization was carried out using a costumed ImageJ macro. The GFP and mCherry spot detection sensitivities were adapted for each marker and strain. The background was subtracted in all images. Cells were segmented and the filters applied were: Median, Remove Outliers and Watershed. Then, particles were analyzed and colocalization was quantified as the area of mCherry spots that overlaps with GFP normalized to the total area of GFP.

Acknowledgements

I thank my project director Dr. Oriol Gallego Moli for his valuable discussions and guidance during the project. I also want to thank Irene Pazos, postdoc in the research group, for providing some of the strains used in the study and for her attentive support. Finally, I thank Radovan Dojcilovic, postdoc in the research group, for his help with the computational correction of the images, all the lab members of the group and the Department of Experimental and Health Sciences of the Universitat Pompeu Fabra for providing the curricular internship agreement.

References

1. Chang IJ, He M, Lam CT. Congenital disorders of glycosylation. Ann Transl Med. 2018 Dec;6(24):477–477.

2. Jaeken J. Congenital disorders of glycosylation. In: Handbook of Clinical Neurology. Elsevier B.V.; 2013. p. 1737–43.

3. Aebi M. N-linked protein glycosylation in the ER. Vol. 1833, Biochimica et Biophysica Acta - Molecular Cell Research. Biochim Biophys Acta; 2013. p. 2430–7.

4. Helenius J, Ng DTW, Marolda CL, Walter P, Valvano MA, Aebi M. Translocation of lipid-linked oligosaccharides across the ER membrane requires Rft1 protein. Nature. 2002 Jan 24;415(6870):447–50.

5. Haeuptle MA, Pujol FM, Neupert C, Winchester B, Kastaniotis AJJ, Aebi M, et al. Human RFT1 Deficiency Leads to a Disorder of N-Linked Glycosylation. Am J

Hum Genet. 2008 Mar 3;82(3):600–6.

6. Koerte A, Chong T, Li X, Wahane K, Cai M. Suppression of the yeast mutation rft1-1 by human p53. J Biol Chem. 1995;270(38):22556–64.

7. Frank CG, Sanyal S, Rush JS, Waechter CJ, Menon AK. Does Rft1 flip an N-glycan lipid precursor? Vol. 454, Nature. Nature Publishing Group; 2008.

8. Sanyal S, Frank CG, Menon AK. Distinct flippases translocate glycerophospholipids and oligosaccharide diphosphate dolichols across the endoplasmic reticulum. Biochemistry [Internet]. 2008 Jul 29 [cited 2021 May 18];47(30):7937–46. Available from: https://pubmed.ncbi.nlm.nih.gov/18597486/

9. Jelk J, Gao N, Serricchio M, Signorell A, Schmidt RS, Bangs JD, et al. Glycoprotein biosynthesis in a eukaryote lacking the membrane protein Rft1. J Biol Chem. 2013 Jul 12;288(28):20616–23.

10. Salari R, Salari R. Investigation of the Best Saccharomyces cerevisiae Growth Condition. Electron physician. 2017 Jan 25;9(1):3592–7.

11. Gottier P, Gonzalez-Salgado A, Menon AK, Liu YC, Acosta-Serrano A, Bütikofer P. RFT1 protein affects glycosylphosphatidylinositol (GPI) anchor glycosylation. J Biol Chem. 2017 Jan 20;292(3):1103–11.

12. Stanley P. Golgi glycosylation. Cold Spring Harb Perspect Biol. 2011 Apr;3(4):1–13.

13. Gietz RD. Yeast transformation by the LiAc/SS carrier DNA/PEG method. Methods Mol Biol. 2014;1205.

14. Janke C, Magiera MM, Rathfelder N, Taxis C, Reber S, Maekawa H, et al. A versatile toolbox for PCR-based tagging of yeast genes: New fluorescent proteins, more markers and promoter substitution cassettes. Yeast. 2004;21(11):947–62.

15. Laughery MF, Hunter T, Brown A, Hoopes J, Ostbye T, Shumaker T, et al. New vectors for simple and streamlined CRISPR-Cas9 genome editing in Saccharomyces cerevisiae. Yeast. 2015 Dec 1;32(12):711–20.

Figures

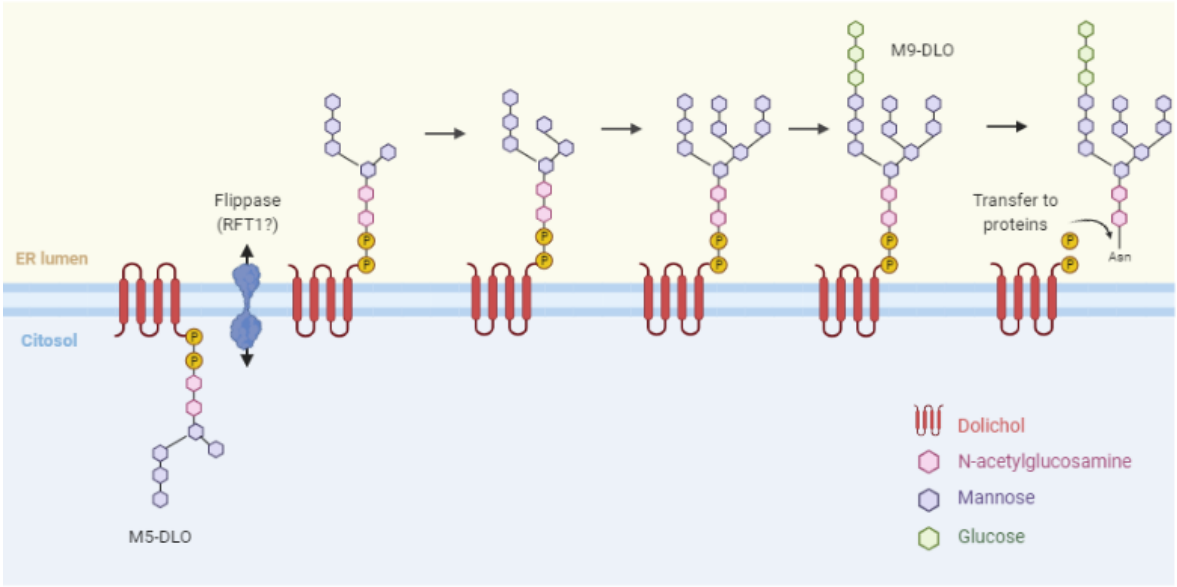

Figure 1. Schematic representation of the N-glycosylation pathway. Biosynthesis of N-linked oligosaccharides starts at the cytoplasmic side of the ER membrane and finishes in the ER lumen. The lipid dolichol serves as a membrane-bound carrier of the oligosaccharides. When M5-DLO is generated on the cytoplasmic side of the ER, RFT1 is proposed to translocate the M5-DLO from the cytoplasmic side to the lumen side of the ER. In the ER lumen, it is extended to mature M9-DLO. Then, M9 glycan is transferred from the lipid carrier to Asn residues of proteins. Adapted from Helenius J. et al, 2002.

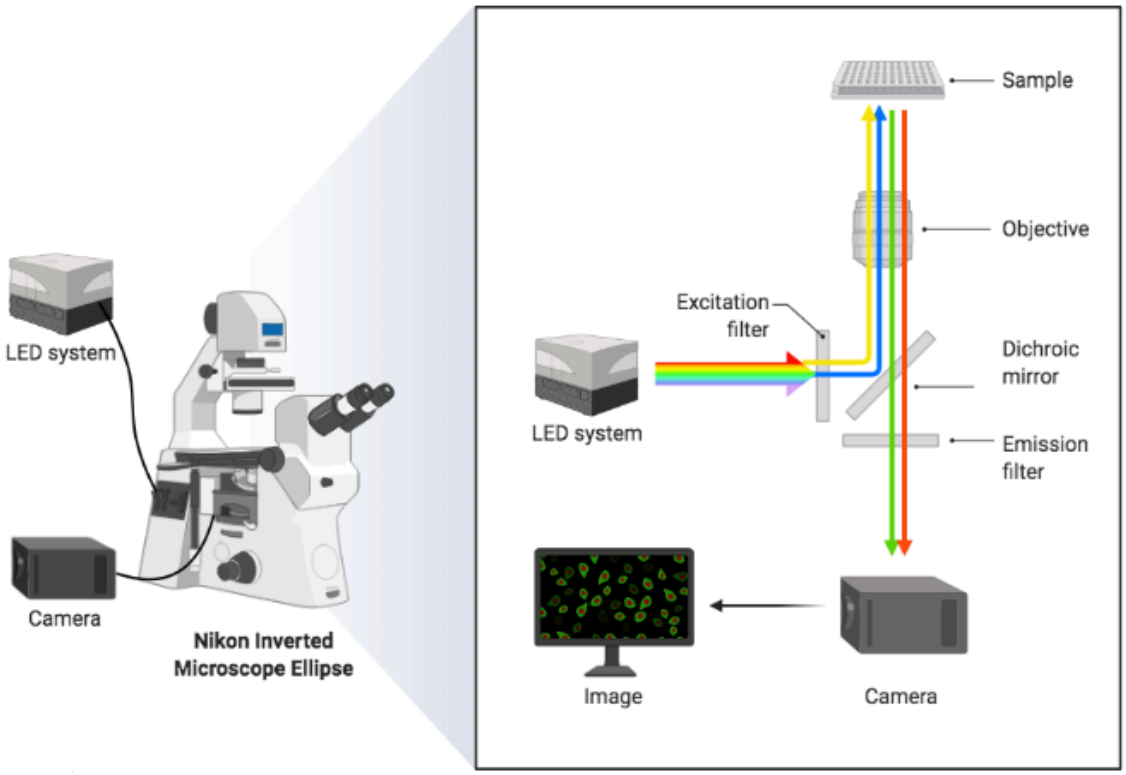

Figure 2. Microscope setup. The sample of interest is illuminated with a LED system through the lens in the objective. The illumination light is filtered by the excitation filter, which lets through light with specific wavelength that matches the fluorophores in the sample. The radiation collides with the dichroic mirror, that reflects excitation wavelengths (cyan and yellow). Light hits the fluorophores in the sample and electrons are excited in a higher level. When they relax, they emit light. The fluorescence emitted by the sample (green and red) is filtered by the emission filter that allows to pass only emission wavelengths. Then, light hits the dichroic mirror that passes emission wavelengths towards the detector (camera).

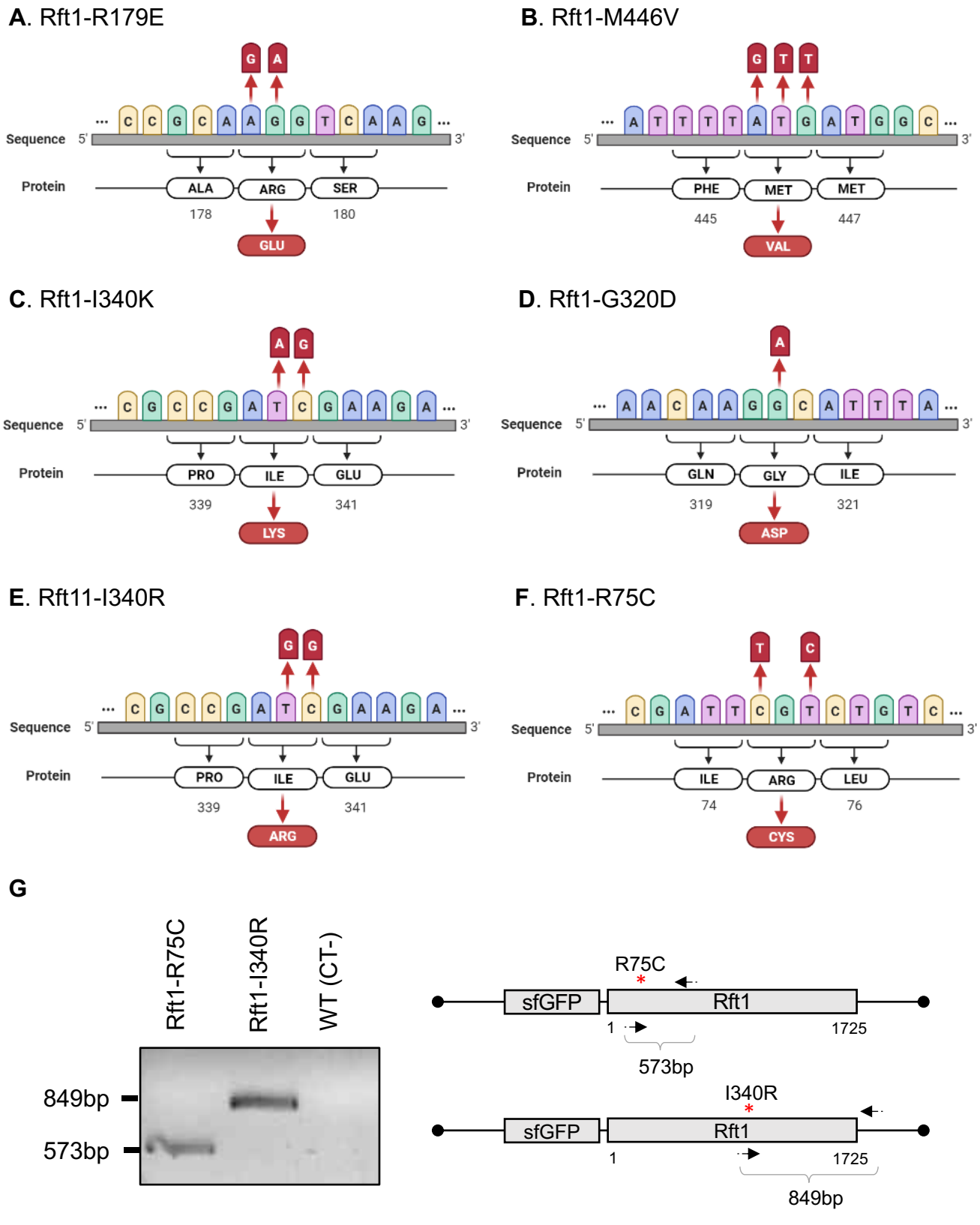

Figure 3. Generation of Rft1-CDG mutant strains. (A-F) Schematic representation of Rft1-CDG mutations generated in yeast using CRISPR/Cas9 technology. Mutated bases and resulting amino acids in red. **(G)** Left, DNA electrophoresis gel of amplified *RFT1* gene with mutation-specific primers for Rft1-R75C and Rft1-I340R mutant yeast strains. *Wild-type* strain was used as a negative control. Right, schema of the expected band size.

A

	HAPLOID CELLS	DIPLOID CELLS	T_D (HOURS)
Rft1 (wt)	✓	-	1.74
Rft1-R179E	✓	-	2.27
Rft1-M446V	✓	-	1.77
Rft1-I340K	✓	-	3.73
Rft1-G320D	✓	-	2.82
Rft1-I340R	-	✓	ND
Rft1-R75C	-	✓	ND

B

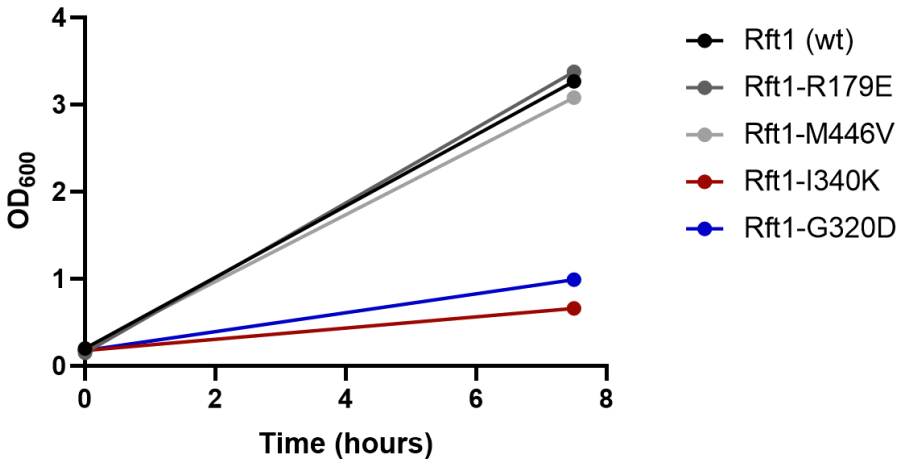

Figure 4. Characterization of Rft1-CDG mutant strains. (A) Table showing Rft1-CDG mutant strains generated either in haploid or diploid cells with the corresponding duplication times. Td, duplication time. ND, not determined. **(B)** Change in OD_{600} of cell culture over 7.5 h in wild-type and Rft1-CDG mutant strains.

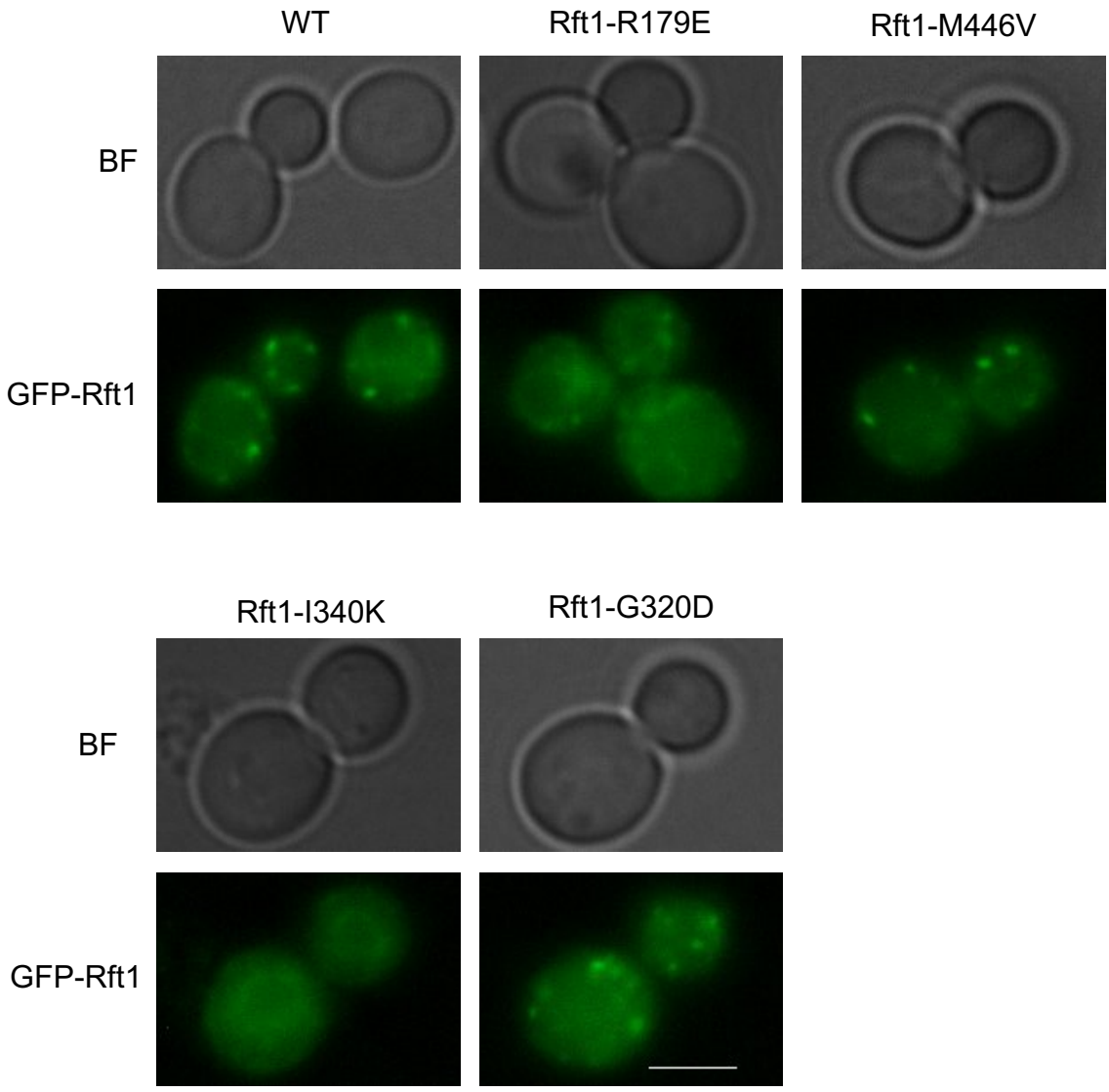

Figure 5. Subcellular distribution of GFP-Rft1. Representative images of GFP-tagged Rft1 in wild-type and in Rft1-CDG mutant strains. BF, brightfield images. Scale bar, 3.22 μm.

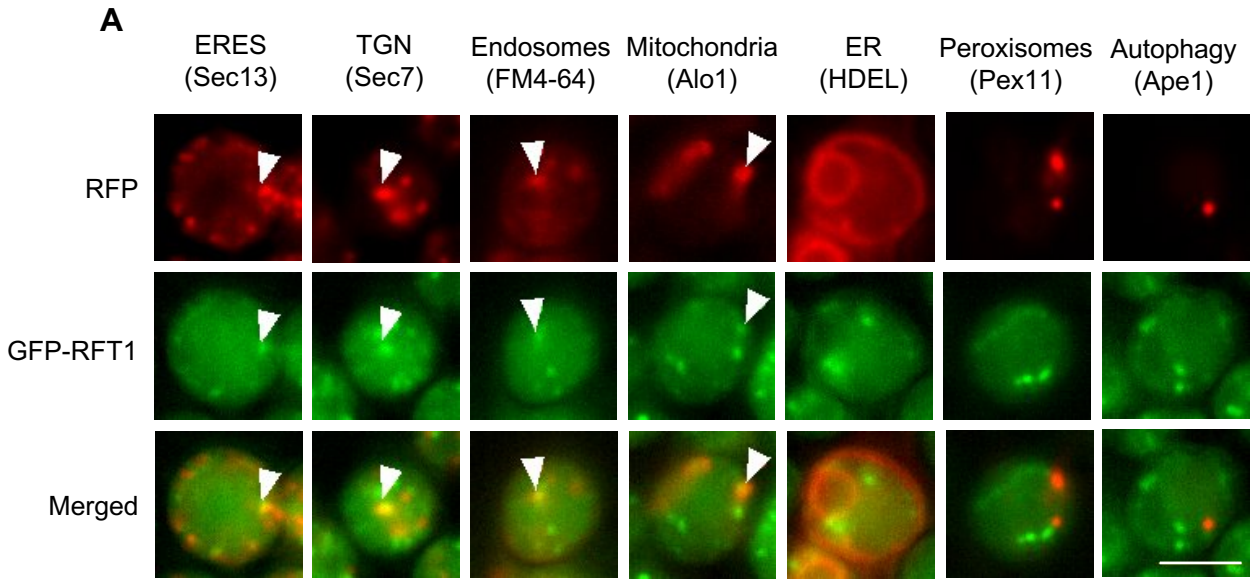

B

	SEC13	SEC7	FM4-64	ALO1	HDEL	PEX11	APE1
%Rft1 (wt)	13.3±3.3	7.8±1.8	5.7±3.6	7.2±2.2	4.2±3.4	0.3±0.1	0

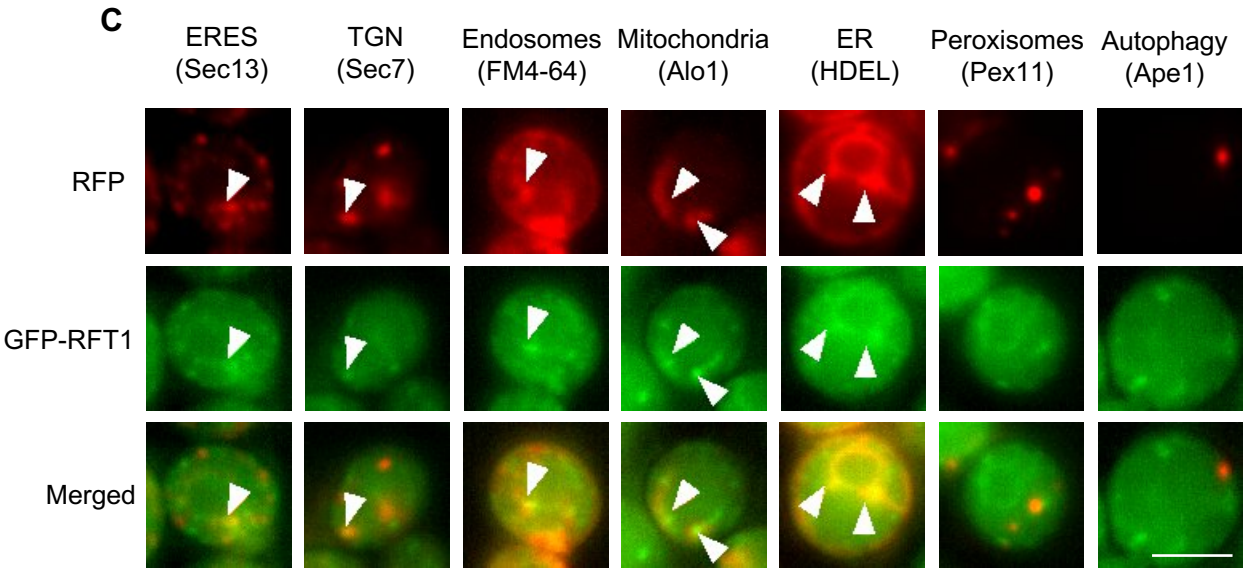

Figure 6. Colocalization analysis of GFP-Rft1 and different cell markers. (A-B) Representative fluorescence images of GFP tagged Rft1 and mCherry tagged subcellular structures in wild-type Rft1 strain. Markers: Sec7 (Trans Golgi Network), Sec13 (ER Exit Sites), Alo1 (Mitochondria), Pex11 (Peroxisomes), HDEL (ER), Ape1 (Selective autophagy) and FM4-64 (Endosomes). Arrowheads point to colocalizing spots. Scale bar, 3.22 μm. **(B)** Table showing quantification of colocalization as the area of overlap between red-labelled structures and GFP normalized to the total area of GFP (Mean ± SD). **(C)** Representative fluorescence images of GFP tagged Rft1 and mCherry tagged subcellular structures in Rft1-R179E mutant strain. Markers: Sec7 (Trans Golgi Network), Sec13 (ER Exit Sites), Alo1 (Mitochondria), Pex11 (Peroxisomes), HDEL (ER), Ape1 (Selective autophagy) and FM4-64 (Endosomes). Arrowheads point to colocalizing spots. Scale bar, 3.22 μm.

Supplementary Materials

PLASMID	TAG	MARKER	SOURCE
pOG044	sfGFP	Ura	Knop
pOG105	HDEL-mCherry	Leu	-
pOG190	Ape1-mCherry	Ura	Vivek Malhotra's group
pOG201	3mCherry	Nat	Kaksonen group
pOG336	pmL_Rft1_R179E	Nat	GenScript
pOG337	pmL_Rft1_G320D	Nat	GenScript
pOG339	pmL_Rft1_R75C	Nat	GenScript
pOG340	pmL_Rft1_E342K, I340K, I340R	Nat	GenScript
pOG341	pmL_Rft1_M446V	Nat	GenScript

Table S1. Plasmids used in this study.

STRAIN	GENOTYPE	SOURCE
OGY0002	MATα, his3Δ1 leu2Δ0 lys2Δ0 ura3Δ0	Invitrogen
OGY1127	MATa, his3Δ1 leu2Δ0 met15Δ0 ura3Δ0, Gal1pr-JSce1/His, GFP-Rft1	Irene Pazos
OGY1137	MATa, his3Δ1 leu2Δ0 met15Δ0 ura3Δ0, Gal1pr-JSce1/His, GFP-Rft1, R179E	Irene Pazos
OGY1138	MATa, his3Δ1 leu2Δ0 met15Δ0 ura3Δ0, Gal1pr-JSce1/His, GFP-Rft1, M446V	Irene Pazos
OGY1161	MATa, his3Δ1 leu2Δ0 met15Δ0 ura3Δ0, Gal1pr-JSce1/His, GFP-Rft1, I340K	Irene Pazos
OGY1162	MATa, his3Δ1 leu2Δ0 met15Δ0 ura3Δ0, Gal1pr-JSce1/His, GFP-Rft1, G320D	Irene Pazos
OGY1165	MATa, his3Δ1 leu2Δ0 met15Δ0 ura3Δ0, Gal1pr-JSce1/His, GFP-Rft1, Sec13-3mCherry Nat	This study
OGY1166	MATa, his3Δ1 leu2Δ0 met15Δ0 ura3Δ0, Gal1pr-JSce1/His, GFP-Rft1, Alo1-3mCherry Nat	This study
OGY1167	MATa, his3Δ1 leu2Δ0 met15Δ0 ura3Δ0, Gal1pr-JSce1/His, GFP-Rft1, Pex11-3mCherry Nat	This study
OGY1170	MATa, his3Δ1 leu2Δ0 met15Δ0 ura3Δ0, Gal1pr-JSce1/His, GFP-Rft1, Sec7-3mCherry Nat	This study
OGY1171	MATa, his3Δ1 leu2Δ0 met15Δ0 ura3Δ0, Gal1pr-JSce1/His, GFP-Rft1, M446V, Sec7-3mCherry Nat	This study
OGY1172	MATa, his3Δ1 leu2Δ0 met15Δ0 ura3Δ0, Gal1pr-JSce1/His, GFP-Rft1, M446V, Sec13-3mCherry Nat	This study
OGY1173	MATa, his3Δ1 leu2Δ0 met15Δ0 ura3Δ0, Gal1pr-JSce1/His, GFP-Rft1, R179E, Sec13-3mCherry Nat	This study
OGY1174	MATa, his3Δ1 leu2Δ0 met15Δ0 ura3Δ0, Gal1pr-JSce1/His, GFP-Rft1, R179E, Alo1-3mCherry Nat	This study
OGY1175	MATa, his3Δ1 leu2Δ0 met15Δ0 ura3Δ0, Gal1pr-JSce1/His, GFP-Rft1, R179E, Pex11-3mCherry Nat	This study
OGY1176	MATa, his3Δ1 leu2Δ0 met15Δ0 ura3Δ0, Gal1pr-JSce1/His, GFP-Rft1, I340K, Alo1-3mCherry Nat	This study
OGY1201	MATa, his3Δ1 leu2Δ0 met15Δ0 ura3Δ0, Gal1pr-JSce1/His, GFP-Rft1, R179E, Sec7-3mCherry Nat	This study
OGY1202	MATa, his3Δ1 leu2Δ0 met15Δ0 ura3Δ0, Gal1pr-JSce1/His, GFP-Rft1, G320D, Alo1-3mCherry Nat	This study

Table S2. Strains used in this study.